

COMPUTER SIMULATION OF EVAPORATIVE COOLING OF BUILDINGS BY WATER SPRAY VAPORIZATION

Antonio César S. Baptista da Silva¹, José A. Bellini da Cunha Neto², Roberto Lamberts³

¹ Federal University of Pelotas /FAUrb/DTC - Brazil: acsbs@ufpel.tche.br;

² Federal University of Santa Catarina / CTC / EMC / LMPT - Brazil: bellini@lmpt.ufsc.br

³ Federal University of Santa Catarina / CTC / ECV / LabEEE - Brazil: lamberts@ecv.ufsc.br

ABSTRACT

This paper presents the performance of a computer simulation code for modelling the evaporative cooling of buildings by water spray vaporization, bring together the scales of the droplet, spray and building. The capability of the models to predict evaporation and building behavior was examined in a series of parametric tests. The parametric explorations have served to demonstrate that the model is sufficiently consistent and react qualitatively well to variations of input parameters.

INTRODUCTION

Evaporative cooling of air is an attractive energy efficient technique for producing a comfortable indoor environment. The efficiency and low cost of water spray evaporative cooling systems makes them a good alternative to reduce the energy use.

Despite this, building simulation software does not incorporate direct evaporative cooling spray models, because an accurate prediction of spray evaporation is difficult due to the complex physical phenomena.

A study was developed that considers the evaporative cooling by microaspiration of water, using a one-dimensional model of spray vaporization that can be easily used in building thermal performance simulations.

Using a discrete particles model with separate flows and solving a non-homogeneous ordinary differential equations system, it was possible to verify the outflow, temperature and humidity of the treated air, at the end of the plume.

The mathematical model of spray was described in Silva et al. (2003), Silva (2004) and Silva et al. (2004). In the first paper, the gas phase Lewis number is assumed to be unity in the droplet model (Faeth, 1977). In the others, as in the present case, the gas phase Lewis number (Le) is **not** assumed to be unity in the droplet model, increasing one equation in the model (Faeth, 1983).

An extensive number of parametric tests were used to check each variable of spray: (1) air velocity; (2) droplets velocity; (3) radius of the droplet; (4) angle

of spray; (5) droplets temperature; (6) air temperature inside the spray; (7) humidity ratio inside the spray; (8) liquid outflow; (9) entrainment air temperature; (10) entrainment air humidity. From these tests it were possible to affirm that the mathematical model of spray (fluid dynamics and heat and mass transfer) is sufficiently consistent. These results were partially presented in Silva et al. (2003) and Silva et al. (2004) and extensively discussed in Silva (2004). In this paper the mathematical model of spray was coupled to a simplified building simulation model. Several parametric tests of the main variables involved are presented.

MATHEMATICAL SPRAY MODEL

The mathematical solution of sprays includes the solution of equations of momentum, energy and mass conservation, for each phase.

It was adopted the *discrete particle model in separate flows*, in which spray is divided into samples of discrete droplets, whose motion and transport are tracked through the flow field, using a Lagrangian formulation, while air is treated through a Eulerian formulation (Faeth, 1983). The effect of droplets on the gas phase is considered by introducing appropriate source terms into the gas phase equations of motion.

From Ghosh and Hunt (1994), there follows the governing equations that define the numerical solution of the dynamic behavior:

- Entrainment law, assuming formally that $c \ll 1$

$$\frac{d}{dz} \pi l_a^2 V_a = 2\pi\beta V_a l_a \quad (1)$$

$$\frac{d}{dz} \pi l_a^2 V_a = \frac{d}{dz} \pi l^2 V_a \quad \text{for } c > 0.194 \quad (2)$$

where the entrainment coefficient β is 0.11 and c is the tangent of the half-angle of spray.

- Volume fraction

$$\alpha = \frac{Q_l}{V_l \pi l^2} \quad (3)$$

where $l = cz$ (4)

- Force on the droplets

$$\frac{F_z}{\rho_a} = -\frac{3}{8a} C_D (V_l - V_a)^2 \alpha \quad (5)$$

where a is the radius of the droplet, ρ_a is the specific mass of air and C_D is the drag coefficient

- Rate of change of the average momentum of droplets

$$V_l \frac{dV_l}{dz} = \left(\frac{F_z}{\rho_a} \right) \left(\frac{\rho_a}{\rho_l} \right) \alpha^{-1} \quad (6)$$

where ρ_l is the specific mass of water.

- Rate of change of momentum flux of the air jet

$$\frac{d}{dz} (\pi l_a^2 V_a^2) = - \left(\frac{F_z}{\rho_a} \right) \pi l^2 \quad (7)$$

At the point where the disruption of the liquid film occurs, the initial droplet velocity equals that of the liquid sheet, and the air jet width (l_a) is approximately equal to the spray width (l_0). At $z=z_0$, the initial conditions are

$$V_a = V_{a_0}; \quad V_l = V_{l_0} \quad \text{and} \quad l_a = l_0 \quad (8)$$

Through the discrete particle model it is possible to analyze the transference of heat and mass between a droplet and the air that surrounds it. It is considered that the conditions of the environment are known and constant during each time interval of the quasisteady process and that the equations are corrected to include the effect of relative movement between the droplet and the air, as suggested by Sirignano (1999) and Faeth (1983).

- Rate of change of the droplet radius

$$\frac{da}{dz} = - \frac{\dot{m}}{4\pi a^2 \rho_l V_l} \quad (9)$$

where \dot{m} is the mass transfer rate from the droplet to the air, corrected for $Re \neq 0$ (Faeth, 1983),

$$\dot{m} = \left\{ 1 + \frac{0.278 Re^{1/2} Sc^{1/3}}{\left[1 + \frac{1.232}{Re Sc^{4/3}} \right]^{1/2}} \right\} \dot{m}_{Re=0} \quad (10)$$

for air under normal conditions of temperature and pressure, Schmidt number (Sc) = ν_a/D_{AB} . The mass transfer rate from droplet to air for $Re = 0$ ($\dot{m}_{Re=0}$) is defined, by Faeth (1983), as

$$\frac{\dot{m}_{Re=0}}{4\pi a \rho_a D_{AB}} = \ln \left[\frac{1 + W_s}{1 + W_a} \right] \quad (11)$$

where D_{AB} is mass diffusivity and W_s is saturation humidity ratio (at droplet surface)

- Rate of change of the droplet temperature

$$\frac{dT_l}{dz} = \frac{3}{4} \frac{\dot{m} H_l}{\pi a^3 \rho_l c_{p_l} V_l} \left[\frac{B_T}{B_Y} Le^{2/3} - 1 \right] \quad (12)$$

where c_{p_l} is the specific heat of the water, H_l is the latent heat of vaporization, Le is Lewis number and B_T and B_Y are

$$B_T = \frac{c_{p_a} (T_a - T_l)}{H_l} \quad (13)$$

and

$$B_Y = \frac{W_s - W_a}{1 + W_a} \quad (14)$$

Following the discrete particle model in separate flows, it was possible to analyze the conservation of mass and energy. At the scale of the spray the volume fraction, α , is used to ponder the variables calculated in the discrete particle model, such as mass flows and outflow that arrive at each control volume.

The control volume ($d\forall$) is defined by equation:

$$d\forall = \pi l^2 dz \quad (15)$$

Considering the evaporation of the droplets, the outflow of liquid, Q_l , will not be constant as a function of z , although the number of droplets remains constant until their complete evaporation. Using conservation laws, the variation of the liquid outflow (Q_l) can be described by the expression:

$$\frac{1}{Q_l} \frac{dQ_l}{dz} = - \frac{3}{4} \frac{\dot{m}}{\pi a^3 \rho_l V_l} \quad (16)$$

Thus, in the one-dimensional model, all the variables are functions only of z and the balance equations can be written as follows:

- Mass vapor conservation

$$\frac{d}{dz} [\rho_a V_a \pi l^2 W_a (1 - \alpha)] - \pi \rho_l W_i \frac{d}{dz} [l^2 V_a] - \frac{3}{4} \frac{\dot{m} Q_l}{\pi a^3 V_l} = 0 \quad (17)$$

where W_a is the humidity ratio of the air inside of the control volume and W_i is the humidity ratio of induced air.

- Energy conservation

$$\frac{d}{dz} [\rho_a V_a \pi^2 h_a (1-\alpha)] - \pi \rho_l h_i \frac{d}{dz} [l^2 V_a] + \rho_l c_p \frac{d}{dz} (T_l Q) = 0 \quad (18)$$

where h_i and h_a are respectively, the enthalpy of the induced air and the enthalpy of the air inside of control volume.

Using this equation system [(1) – (18)], and other complementary equations, it was possible to verify the outflow, temperature and humidity of the treated air, at the end of the plume. These output data were used to simulate the thermal performance of buildings.

COUPLING THE SPRAY MODEL TO A BUILDING MODEL

The physical properties of the air mass, resultant of the contact with the drops, constitute the term of connection between spray and building, when the evaporation of the drops is completed. Figure 1 represents the iteration between spray and the environment, where the air outflow of the spray model constitutes data for input to the building model and surrounding air is a variable, at each time step, for the spray model.

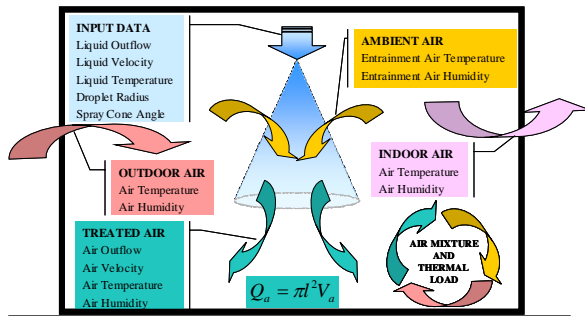


Figure 1 Schematic diagram of coupling model

Thus, between the solution of spray and the evaluation of the building behavior exists a process of mixture of air masses at different conditions of temperature and humidity. The indoor and outdoor air and the treated air outflow for the nozzles interact at each time step with the sources of sensible and latent loads of the building. Figures 2 and 3 show schematically the conditions of the physical states of air masses. As the process occurs simultaneously, this sequence of mixture of air masses is merely an illustration.

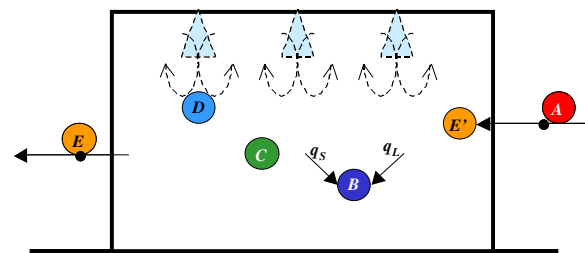


Figure 2 Schematic diagram of evaporative cooling

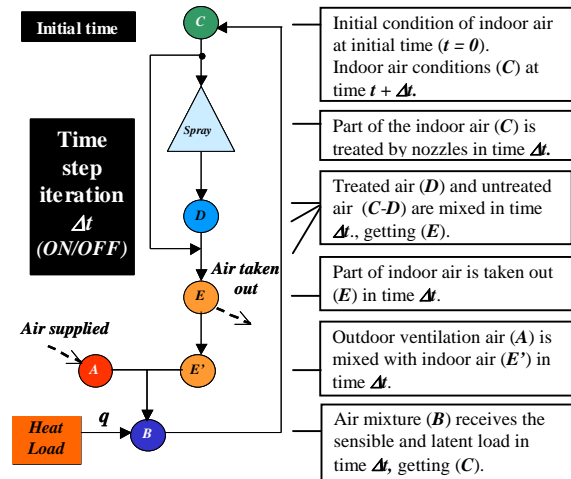


Figure 3 Schematic flowchart of evaporative cooling

The interval of time, Δt , represents the ON and/or OFF time of spray calculated from user configuration controls and thresholds. Users can pre-define environmental settings including temperature and humidity set points and dead bands.

The treated air outflow, while spray (or set of sprays) was ON, is, then, mixed with indoor air and the ventilation air. The changes in sensible and latent load are computed and brought up to date as a function of time of spray ON and/or OFF. The implementation of the models was made in FORTRAN Power Station 4,0 and has considered all the variables intervening in the performance of building cooled by water spray vaporization.

Four modules compose the program:

- Main Program
- Environment Sub-routine
- Controller Sub-routine
- Spray Sub-routine

Main Program manages the entrance and exit of data and activates the Controller and Environment sub-routines.

Controller sub-routine determines the time (ON/OFF) of the microaspersión system, as a function of the parameters determined by the user.

Environment sub-routine calculates indoor temperature and humidity that result from thermal loads and the mixture of ventilation and air masses treated by the nozzles. This sub-routine activates the Spray sub-routine when the indoor temperature and humidity conditions point to evaporative cooling system.

Spray sub-routine solves the system of equations to obtain the treated air outflow and its properties at the end of the plume. For a lack of space, the mass and energy balance equations for the room air have been omitted.

RESULTS

A building with 200m² using evaporative cooling was simulated. General characteristics of the base

case building are listed in Table 1, whose outdoor design conditions and thermal loads are the same presented in ASHRAE (1995) to simulate an indirect evaporative cooling system.

Table 1 Base case general characteristics

Building design conditions	Area: 200 m ² Ceiling high: 7 m Air change rate: 10 h ⁻¹ Sensible Heating Load : 48 kW Latent Heating Load: 6 kW Number of nozzles: 20
Outdoor design conditions	Altitude: 0 m (at sea level) Dry bulb temperature: 35°C Relative humidity: 18%
Set up conditions	Maximum indoor temperature (T_{max}): 28°C Minimum indoor temperature (T_{min}): 22°C Maximum indoor humidity (RH_{max}): 80% Minimum indoor humidity (RH_{min}): 50% Maximum time ON (ON_{max}): 60 s Minimum time ON (ON_{min}): 30 s Maximum time OFF (OFF_{max}): 60 s Minimum time OFF (OFF_{min}): 30 s Temperature Dead Band: 2°C Relative Humidity Dead Band: 5%

A typical spray nozzle, normally adopted for evaporative cooling of buildings, was used in building simulation. These characteristics are summarized below:

- Atomization pressure: 5,500 to 6,900 kPa.
- Plain orifice of 0.2 mm diameter
- Droplets Sauter Mean Diameter: 11 micron
- Initial droplets velocity: $V_l = 83.2$ m/s
- Spray cone angle of 60°.
- Initial liquid outflow: $Q_l = 1.567 \times 10^{-6}$ m³/s

Parametric tests were used to check each variable of evaporative cooling of model: (1) number of nozzles (NN); (2) air change rate (n); (3) altitude ($Alt.$); (4) outdoor air temperature (T_e); (5) outdoor relative humidity (RH_e); (6) time settings (ON_{max} , ON_{min} , OFF_{max} , OFF_{min}); (7) sensible heat load (q_s); (8) latent heat load (q_l). Some of these results are shown to illustrate the model. Figures 4 to 6 show the results of base case.

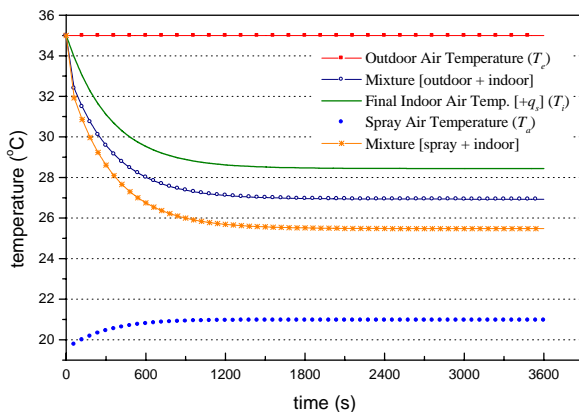


Figure 4 Base case temperatures

As initial condition, the indoor and outdoor temperatures and humidities were considered equal and, at the first moment, the microaspersion system is considered OFF.

In the next steps of the process, the microaspersion system is ON. It treats a part of the indoor air and mixes this air mass dealt with untreated indoor air mass. This air mixture is in turn mixed to the outdoor ventilation air that enters the building. In last stage, this mixture receives the sensible and latent load from the construction, up dating the indoor temperature (T_i), which is shown in Figure 4.

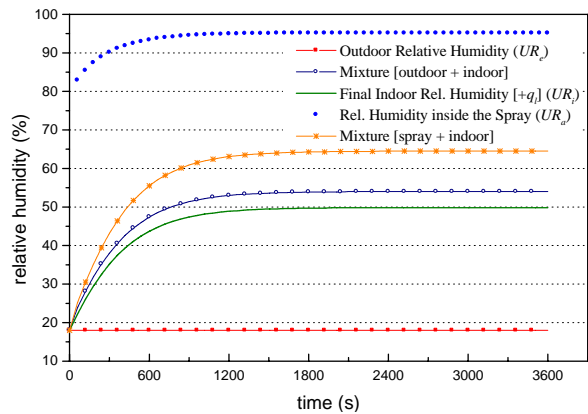


Figure 5 Base case humidities

Figure 5 shows that relative humidities, of each of the stages, present inverse behavior in relation to the temperature.

Figure 6 shows the distance reached by the spray before total evaporation of the droplets. It can be noticed that the penetration of spray grows as the temperature diminishes and the humidity increases, stabilizing at 1.29 m when these variables became constant.

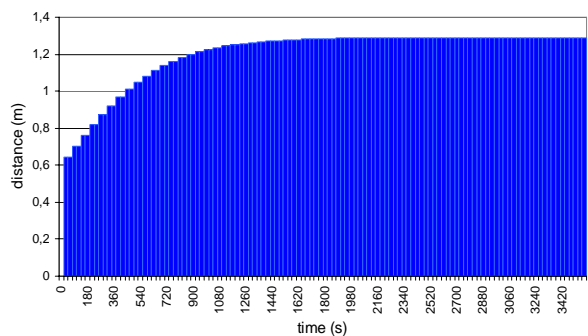


Figure 6 Distance reached by spray

The average temperature and humidity in the period was 29,05°C and 46,88% , respectively, and the system was ON constantly in all the simulated period. Thus, in this specific case, the microaspersion system did not get at the set up conditions, whose temperature should be between 22°C and 28°C and humidity between 50% and 80%.

The list of parametric tests is presented in Table 2.

Table 2 List of parametric tests

VARIABLES	BASE CASE	CASE 01	CASE 02	CASE 03	CASE 04	CASE 05	CASE 06	CASE 07	CASE 08
Alt. (m)	0	0	0	1500	0	0	0	0	0
T_e (°C)	35	35	35	35	35	28	35	35	35
RH _e (%)	18	18	18	18	50	50	18	18	18
n (h ⁻¹)	10	10	6	10	10	10	6	10	10
NN (unid.)	20	25	20	20	20	20	20	20	20
q _s (kW)	48	48	48	48	48	48	48	24	24
q _l (kW)	6	6	6	6	6	6	6	6	12
ON _{max} (s)	60	60	60	60	60	60	120	60	60
ON _{min} (s)	30	30	30	30	30	30	60	30	30
OFF _{max} (s)	60	60	60	60	60	60	120	60	60
OFF _{min} (s)	30	30	30	30	30	30	60	30	30

In case 01 the number of nozzles was modified from 20 to 25. The comparative results are shown in Figures 7, 8 and 9.

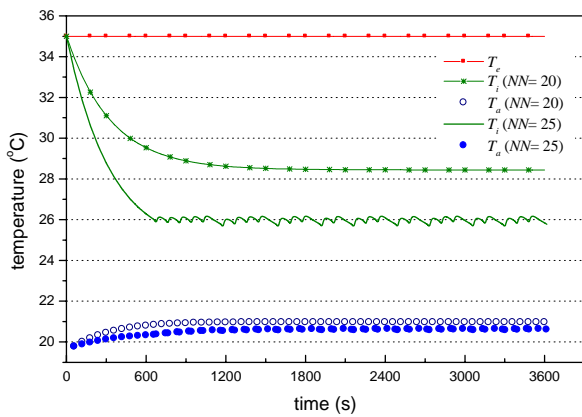


Figure 7 Nozzles number effect on temperature

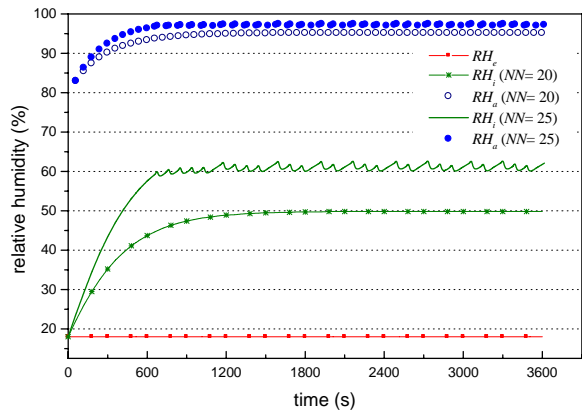


Figure 8 Nozzles number effect on air humidity

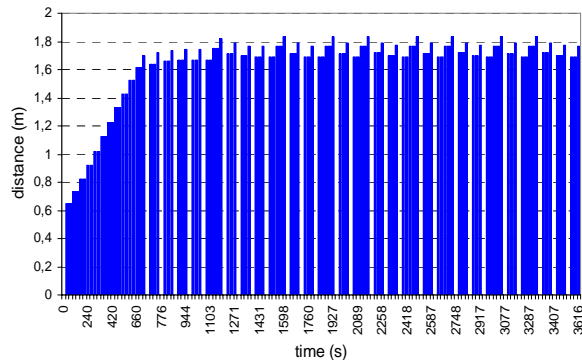


Figure 9 Distance reached by spray (case 01)

The average temperature and relative humidity were 26.42°C and 58.45%, respectively. Figures 7 and 8 show that after 688 seconds the system started an intermittent regimen (ON/OFF). It can be observed in Figure 9 that the spray penetration increases as a function of the reduction of the temperature and increase of the humidity. The blank spaces in Figure 9 indicate the period where the system was off.

In case 02 the air change rate was modified from 10 to 6.

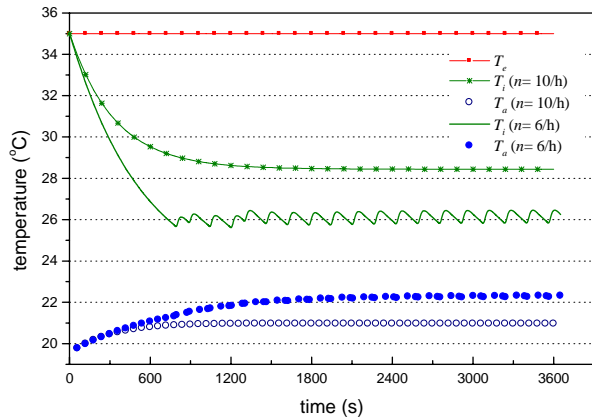


Figure 10 Effect of air change rate on temperature

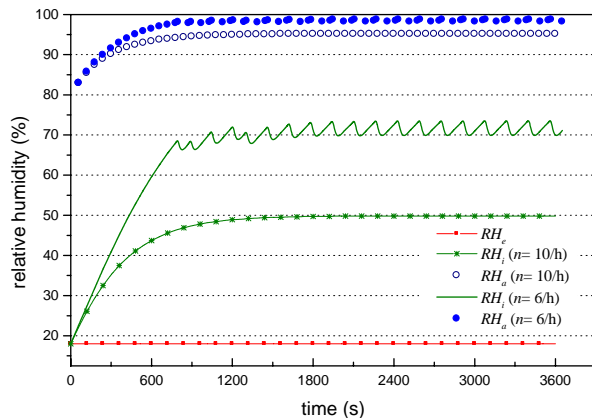


Figure 11 Effect of air change rate on air humidity

Through Figures 10 and 11, it can be observed that the reduction of the outdoor air change rate favored the performance of the system. The average temperature and relative humidity were 26.68°C and 66.17%, respectively.

Case 03 tested the altitude effect on evaporative cooling system changing from sea level to 1500 meters.

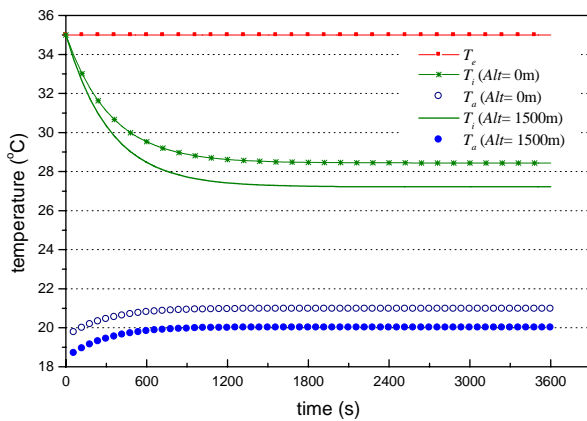


Figure 12 Altitude effect on temperature

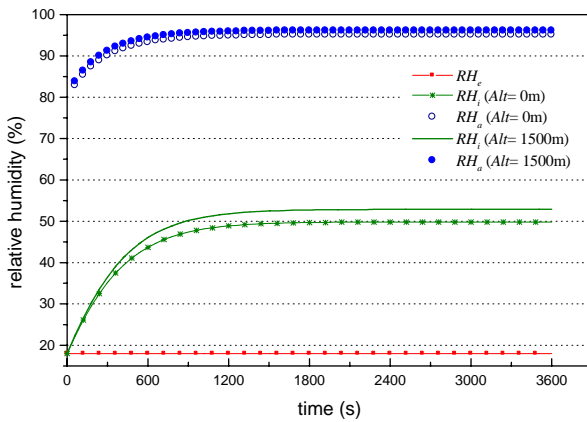


Figure 13 Altitude effect on relative humidity

Figures 12 and 13 show that indoor temperature and spray temperature are reduced, while relative humidities get higher, when the system is used in higher altitudes because, under lower atmospheric pressure, there is an increment of the mass flow (\dot{m}) as function of the increase of W_s and D_{AB} and a reduction of the air density (ρ_a).

Cases 04 and 05 evaluate the system under different outdoor temperature and humidity conditions. These cases are also compared to the *base case*.

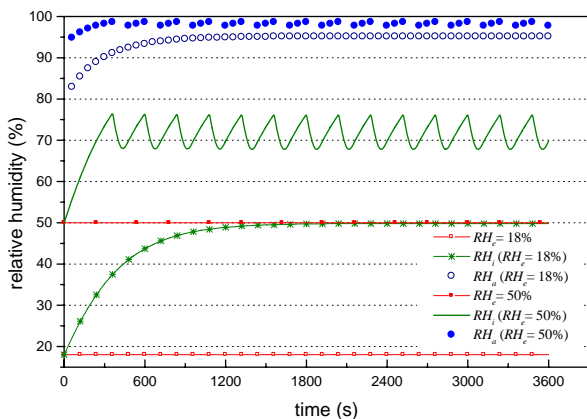


Figure 14 Effect of outdoor conditions on air humidity ($T_e = 35^\circ\text{C}$; $RH_e = 50\%$)

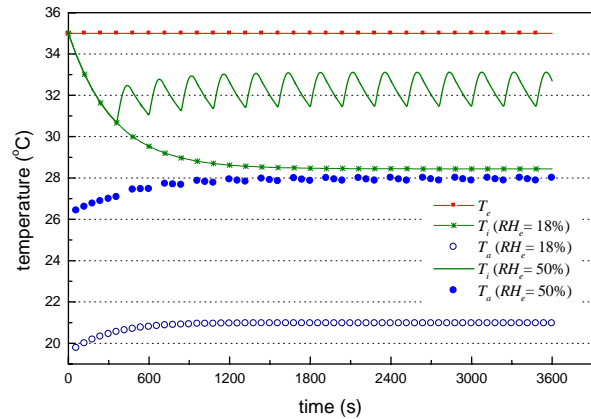


Figure 15 Effect of outdoor conditions on temperature ($T_e = 35^\circ\text{C}$; $RH_e = 50\%$)

Figures 14 and 15 show that the increase of the relative humidity combined with the high internal thermal load resulted in an average indoor temperature of 32.2°C , limited by humidity set point and dead band.

In case 05, the system simulates a situation where the outdoor conditions are near to the comfort requirements ($T_e = 28^\circ\text{C}$; $RH_e = 50\%$), and the system has only to attend the thermal load. Figures 16 and 17 show that the average temperature and relative humidity were 26.64°C and 71%, respectively.

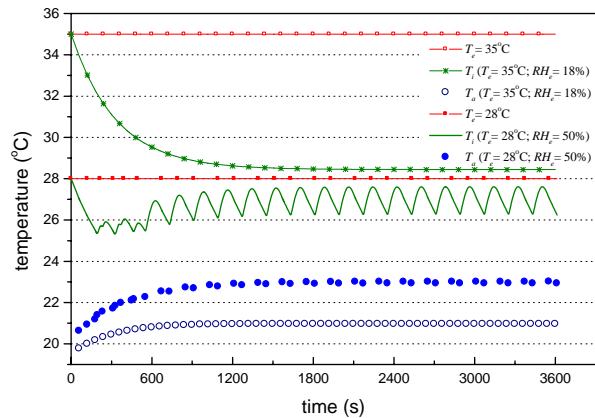


Figure 16 Effect of outdoor conditions on temperature ($T_e = 28^\circ\text{C}$; $RH_e = 50\%$)

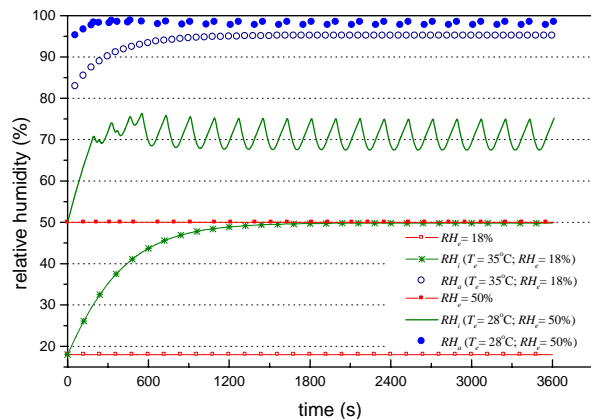


Figure 17 Effect of outdoor conditions on air humidity ($T_e = 28^\circ\text{C}$; $RH_e = 50\%$)

The controller settings intervene in the behavior of the system. Long times of spray ON (ON_{max}) can generate condensation or saturation in the environment. The same problem occurs when the OFF time is large (OFF_{max}), making the temperature of the environment to raise too much in the interval. In case 06 the values of time settings are modified and compared with case 02.

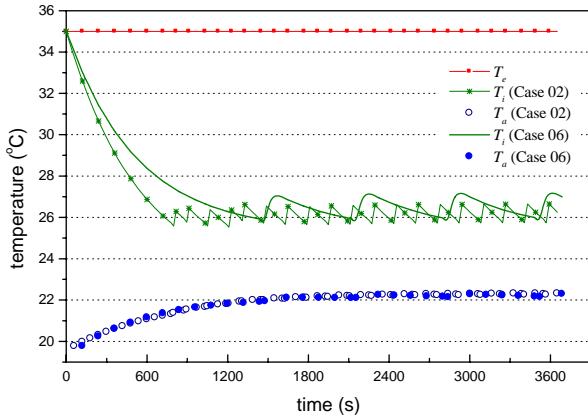


Figure 18 Time settings effect on temperature

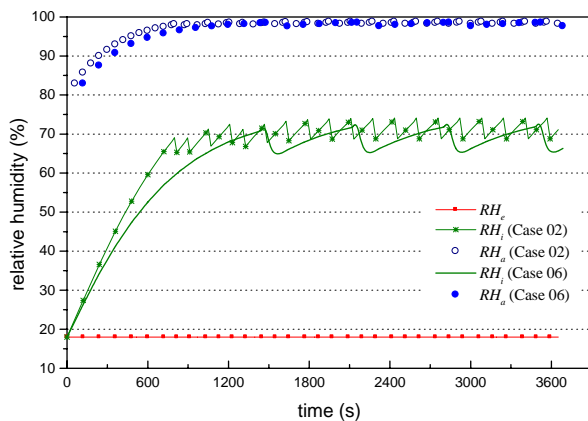


Figure 19 Time settings effect on humidity

Figure 18 and 19 show that average temperature and relative humidity in both cases are similar (difference of only 2 and 5 percent points, respectively). However the computational time of case 02 is much higher than case 06, when the spray module is brought into action with less frequency.

At last, the effect of the thermal loads of the construction, those have obvious effect on any cooling system, will be evaluated in cases 07 and 08.

Figure 20 shows that the reduction of the sensible heat load made the temperature lower quickly and reach the average of 25,75°C. Periods ON/OFF are so short that oscillation of temperature is not perceived during the intermittent period. This indicates that the range time could be reviewed to prevent that the system turn on and turn off many times in a short period of time.

In case 08 latent heat load is modified in relation to case 07 from 12kw to 6 kW.

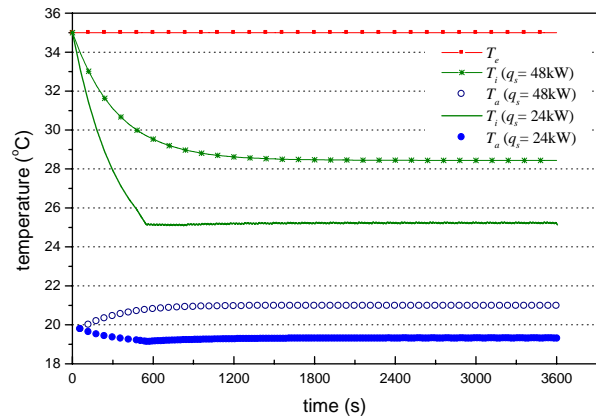


Figure 20 Sensible heat load effect on temperatures

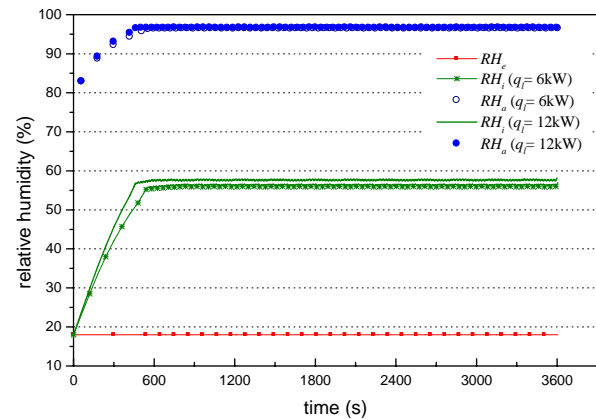


Figure 21 Latent heat load effect on humidities

It was not identified significant changes from case 07 to 08 (Figure 21), although the value of the latent heat load was duplicated. The main reason is the high number of air changes with hot and dry air that come from the exterior.

CONCLUSIONS

These cases show the complexity of simulating the behavior of evaporative cooling of buildings by water spray vaporization. Innumerable combinations of variables and values, from droplet size to set up conditions can equally result in many possibilities of adequacy or not of the system to the context of the climatic and built environment.

The set of cases does not have another purpose than to demonstrate how a thermal simulation of buildings code could incorporate the model of spray to simulate the system of evaporative cooling for microaspersión. The parametric explorations have served to demonstrate that the model is sufficiently consistent and react qualitatively well to variations of input parameters. The coupled model makes possible:

- to design microaspersión systems for cooling and/or humidification of buildings;

- to provide the necessary empirical data needed to design the ventilation system properly, with lesser consumption of water and energy;
- to determine the viability in spray penetration, so as to avoid humidifying objects near the nozzles;
- to measure the water and energy consumption from the consumption of pressure pump and water outflow of each one of the nozzles, weighed by ON/OFF time;
- to analyze the cost/advantage relation of the microaspiration system;
- to evaluate each one of the intervening variables in the process and in the applicability of the microaspiration systems, exploring potential and the possibilities of association with ventilation and air conditioning systems, in diverse climatic environments, types and uses of buildings;
- to contribute with a research area that was restricted by the complexity of the phenomenon;
- to help the development of enthalpy controllers for association between microaspiration and air conditioner systems in different climatic regions;

ACKNOWLEDGMENT

The development of this work was supported by – CAPES – Ministry of Education – Brazilian Government.

NOMENCLATURE

a	radius of the droplet (m)
Alt	altitude (m)
b	arbitrary coefficient
c	tangent of the half-angle of spray
C_D	drag coefficient
c_p	specific heat (kJ/kg.K)
D_{AB}	mass diffusivity (m ² /s)
F_z	average force per unit volume (N/m ³)
h	enthalpy (kJ/kg)
H_l	latent heat of vaporization (kJ/kg)
l	radius of spray jet (m)
l_a	radius of air jet (m)
\dot{m}	mass flow (kg/s)
n	air change rate (h ⁻¹)
NN	number of nozzles
\dot{q}	heat flow at droplet surface (kW/m ²)
Q	volumetric outflow (m ³ /s)
q_s	sensible heat load (kW)
q_l	latent heat load (kW)
RH	relative humidity (%)
Sc	Schmidt number
T	temperature (°C)
V	velocity (m/s)
W	humidity ratio (kg/kg)
z	vertical distance from nozzle (m)
α	volume fraction

β	entrainment coefficient
ρ	specific mass (kg/m ³)
ν	kinematic viscosity (m ² /s)

Subscripts

a	air inside of the control volume
e	outdoor conditions
l	liquid
i	induced air, indoor conditions
s	saturation, droplet surface
0	initial condition

REFERENCES

- ASHRAE. *Chapter 47, Evaporative Air Cooling*, ASHRAE Applications Handbook, 1995. Atlanta: American Society of Heating, Refrigerating and Air-conditioning Engineers, Inc. New York, NY.
- ASHRAE. Psychrometrics – Theory and Practice, 1996, ASHRAE Research Project, 1995. Atlanta: American Society of Heating, Refrigerating and Air-conditioning Engineers, Inc. New York, NY.
- Faeth, G.M. 1977. Current status of droplet and liquid combustion. Progress in Energy and Combustion Science, No. 3, pp. 191 – 224.
- Faeth, G.M. 1983. Evaporation and combustion of sprays. Prog. Energy Combust. Sci., vol. 9, pp. 1-76.
- Ghosh, S., Hunt, J.C.R., 1994. Induced air velocity within droplets driven sprays. Proc. R. Soc. Lond. A 444, pp. 105-127.
- Silva ACSB, Cunha Neto JAB, Lamberts R. 2003. Spray Vaporization for Evaporative Cooling of Buildings. In: *EIGHTH INTERNATIONAL IBPSA CONFERENCE, 2003, Eindhoven. Proceedings of Eighth International IBPSA Conference..* pp. 1209-1216.
- Silva, ACSB. 2004. Simulação de Resfriamento Evaporativo por Microaspersão D'Água. 197p. Doctor Thesis – Program of Post Graduation in Civil Engineering, Federal University of Santa Catarina – Brazil/ SC. (in Portuguese)
- Silva ACSB, Cunha Neto JAB, Lamberts R. 2004. Modelling Spray Vaporization for Evaporative Cooling of Buildings: *Building Service Engineering Research and Technology Volume 25, 4*; pp. 351-361
- Sirignano WA. 1999. *Fluid dynamics and transport of droplets and sprays*. Cambridge University Press, Cambridge, UK.